

DEFLECTION PROFILES OF A MONOENERGETIC ATOMIC BEAM CROSSING A STANDING LIGHT WAVE

C. TANGUY, S. REYNAUD, M. MATSUOKA * and C. COHEN-TANNOUJJI

*Laboratoire de Spectroscopie Hertzienne de l'Ecole Normale Supérieure, et Collège de France,
F 75231 - Paris Cedex 05, France*

Received 14 October 1982

We calculate the shape of the deflection profile of a monoenergetic atomic beam crossing a laser standing wave, in a situation where many spontaneous emission processes occur during the interaction time. We predict that double peaked structures appear when the laser is detuned from resonance.

1. Introduction

During the last few years, the deflection of an atomic beam by a resonant standing laser wave has received a lot of attention. From an experimental point of view, the deflection profile (i.e. the intensity of the deflected beam versus the deflection angle) has been observed on a thermal sodium beam and the laser power dependence of the width of the deflection curve has been investigated [1,2] (see also [3]).

Several theoretical papers have been devoted to the interpretation of such an experiment, starting from the atomic equations of motion and introducing various types of approximations [4–12]. The main purpose of these papers was to understand the variations of the width of the deflection profile with various parameters such as the laser power, the detuning and the interaction time.

In this letter, we would like to point out the interest of studying the deflection profile itself when the atomic beam is monoenergetic. We show that it exhibits important changes when the laser is tuned through resonance: starting from a single maximum curve at exact resonance, the deflection profile changes into a double-peaked structure when the laser is detuned. Our analysis of the deflection profiles in-

cludes situations where the atomic displacement along the standing wave cannot be neglected. This allows us to determine the optimal conditions for getting the largest possible structure.

2. Situation considered in this paper. Notations

All atoms of the beam are supposed to have the same velocity v_0 , parallel to the z axis. They cross at right angle the laser standing wave propagating along the x axis. We take the electric field equal to $E(x, t) = E_0 \cos kx \cos \omega_L t$ in the interaction zone $0 < z < l$ and zero elsewhere. The detuning is $\delta = \omega_L - \omega_0$ and

$$\omega_1(x) = -(dE_0 \cos kx)/\hbar \quad (1)$$

is the spatially varying Rabi frequency (d being the atomic dipole moment). The time of flight $T = l/v_0$ of atoms through the laser beam is the interaction time. We will suppose in this paper that

$$\Gamma T \gg 1, \quad (2)$$

where Γ is the natural width of the upper atomic state. Condition (2), which corresponds to most experimental situations [1,2], means that many spontaneous emission processes occur during the interaction time.

All subsequent calculations will be performed in the initial atomic rest frame moving with velocity v_0 along the x axis.

* Permanent address: Department of Physics, Kyoto University, Kyoto 606, Japan.

3. Fokker–Planck equation for the atomic motion

We will suppose that during its lifetime Γ^{-1} , the atom does not move appreciably in comparison with the wavelength λ of the radiation characterizing the spatial variation of the light intensity. This condition $v\Gamma^{-1} \ll \lambda$, where v is the atomic velocity along the x -axis (due to an imperfect collimation of the atomic beam or to a transfer of momentum from the laser beam), is equivalent to

$$kv \ll \Gamma, \quad (3)$$

which is the usual condition for the “adiabatic approximation”: during its radiative lifetime, the atom experiences a nearly constant light intensity. As a consequence of (2) and (3), one shows that the mean force [13] experienced by an atom at point x is given by

$$f(x) = -dU(x)/dx, \quad (4)$$

where

$$U(x) = (\hbar\delta/2) \log(1 + s(x)) \quad (5)$$

is the potential “seen” by the atom and

$$s(x) = 2\omega_1^2(x)/(\Gamma^2 + 4\delta^2) \quad (6)$$

is the saturation parameter. Because of spontaneous emission, the force exerted by the light wave fluctuates; this leads to an atomic momentum diffusion. We refer the reader to references [14,15] for a correct calculation of the diffusion coefficient. From their results, one derives the following diffusion coefficient along the x axis

$$D(x) = \frac{\hbar^2 \Gamma}{16s(1+s)^3} \left(\frac{ds}{dx} \right)^2 \times \left\{ 1 + (4r-1)s + 3s^2 + \frac{s^3}{r} \right\} + \frac{\hbar^2 k^2}{10} \Gamma \frac{s}{1+s}, \quad (7)$$

where $r = \Gamma^2/(\Gamma^2 + 4\delta^2)$ is the resonance parameter.

A convenient quantum description of the translational degrees of freedom of the atom makes use of the so-called “Wigner distribution” $w(x, p, t)$, where p is the momentum along the x axis [17]. When conditions (2) and (3) are fulfilled, the Wigner distribution can be shown to obey a Fokker–Planck type equation [11,12,18–20]

$$\left[\frac{\partial}{\partial t} + \frac{p}{M} \frac{\partial}{\partial x} + f(x) \frac{\partial}{\partial p} - D(x) \frac{\partial^2}{\partial p^2} \right] w(x, p, t) = 0. \quad (8)$$

The second term of eq. (8) describes the free flight of the atom along the x direction (in the rest frame defined in sect. 2). The last two terms respectively describe the “drift” due to the mean force and the “diffusion” associated with the fluctuations of the force (we neglect the velocity dependent friction forces since we suppose throughout this paper the interaction time T shorter than the “thermalization” one).

4. Deflection profiles when free flight is neglected

We suppose in this section that, during the interaction time T , the atom does not move appreciably along the standing wave, even if it gets some momentum in this direction from the light beam. This restriction will be removed in sect. 5. The corresponding condition $vT \ll \lambda$ or

$$kv \ll T^{-1} \quad (9)$$

is more stringent than the adiabatic condition (3), as a consequence of (2).

When (9) is fulfilled, one can ignore the free flight term $(p/M)\partial/\partial x$ in the Fokker–Planck equation (8) which becomes local in x and then admits the following solution

$$w_{\text{out}}(x, p) = \int dq w_{\text{in}}(x, p - q)G(x, q, T), \quad (10)$$

where w_{in} and w_{out} are the Wigner distributions for $t = 0$ and $t = T$ respectively and where $G(x, q, T)$ is the well-known Green function of a second order differential equation in p

$$G(x, q, T) = [4\pi TD(x)]^{-1/2} \times \exp[-(q - Tf(x))^2/4TD(x)]. \quad (11)$$

From (10), it appears that such a Green function can be considered as a probability distribution for the momentum q transferred during the time T to an atom located at a point x . Strictly speaking, such a picture violates the Heisenberg relation for x and p . This is due to the fact that the Green function does not describe a physical state. Actually, the physical

states are described by Wigner distributions satisfying the Heisenberg relation.

As a next step, we now suppose that the initial distribution in p is much narrower than the distribution of the momentum transfer q , so that eq. (10) becomes

$$w_{\text{out}}(x, p) = G(x, p, T) \int dq w_{\text{in}}(x, p - q) = G(x, p, T) X_{\text{in}}(x), \quad (12)$$

where $X_{\text{in}}(x)$ is the probability for the atom to be initially at position x . One gets the momentum distribution by integrating (12) over x

$$P_{\text{out}}(p) = \int dx w_{\text{out}}(x, p) = \int dx G(x, p, T) X_{\text{in}}(x). \quad (13)$$

$G(x, p, T)$ thus appears (with the same restrictions as above) as the distribution of the final momentum of an atom crossing the laser beam at point x . According to (11), $G(x, p, T)$ is a normal distribution in p (gaussian shape), centered at

$$\bar{p}(x) = Tf(x) \quad (14)$$

and having a dispersion

$$\Delta p^2(x) = \overline{p^2(x)} - \bar{p}^2(x) = 2TD(x). \quad (15)$$

Eq. (13) expresses that the deflection profile is obtained by superposing such gaussian curves corresponding to different values of x .

Finally, since $G(x, p, T)$ is, as $f(x)$ and $D(x)$, a periodic function of x (period $\lambda/2$), and since the width of $X_{\text{in}}(x)$ is much larger than λ , we can write

$$P_{\text{out}}(p) = \frac{2}{\lambda} \int_{-\lambda/4}^{+\lambda/4} dx G(x, p, T). \quad (16)$$

Fig. 1 represents deflection profiles [$P_{\text{out}}(p)$ versus p] computed for various values of the detuning δ .

For a resonant excitation ($\delta = 0$), one gets a single peak centered around $p = 0$ (curve a). This is due to the fact that the Green functions appearing in (16) are gaussian curves in p with different widths, but all centered on $p = 0$ [$f(x) \equiv 0$ for $\delta = 0$; see eq. (5)]. Their superposition therefore gives a bell-shaped profile.

For a non resonant excitation, $P_{\text{out}}(p)$ exhibits

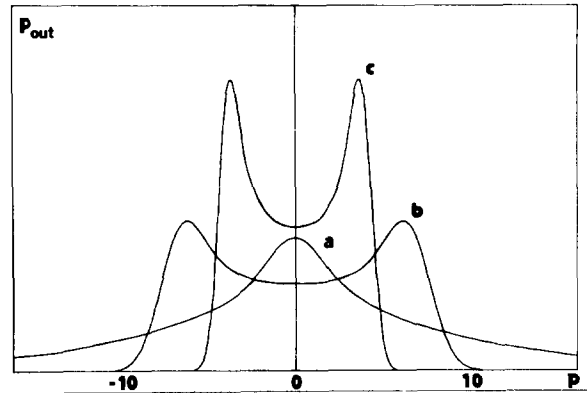


Fig. 1. Deflection profiles ($P_{\text{out}}(p)$ versus p in units of hk) for various values of the detuning: $\delta = 0$ (curve a), $\delta = -5\Gamma$ (b), $\delta = -10\Gamma$ (c). Calculations have been performed for sodium atoms with a Rabi frequency $dE_0/\hbar = 5\Gamma$ and an interaction time $T = 7\Gamma^{-1}$. With these parameters, free flight can be neglected.

two maxima for sufficiently large values of δ (fig. 1, curves b and c). In order to understand such a structure, consider the values $\bar{p}(x_i)$ corresponding to points x_i equally spaced on the x axis. Fig. 2 clearly shows that they are not uniformly distributed. They rather bunch near the two extrema $\pm p_M$. When summing the gaussian curves centered on $\bar{p}(x_i)$, a greater number of values of x_i will contribute to deflections in the neighbourhood of $\pm p_M$ than for $p = 0$. Such a graphical construction clearly explains why the deflection profile exhibits two maxima near $\pm p_M$ (provided that p_M is larger than the width of the gaussian curves).

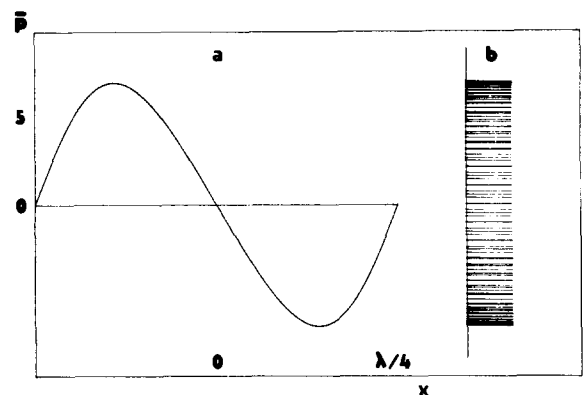


Fig. 2. (a). Mean momentum $\bar{p}(x) = Tf(x)$ versus x (same parameters as for fig. 1b). (b). Distribution of the $\bar{p}(x_i)$'s for equally spaced values of x_i . Bunchings appear near the two extremal values $\pm p_M$.

When the detuning δ is too large, the gradient force tends towards zero (it varies with δ as a dispersion shaped curve) and one understands why the distance between the two maxima $\pm p_M$ decreases (fig. 1, curve c).

5. Free flight taken into account

In order to increase the distance $2p_M$ between the two peaks of the deflection profile, one can try to increase the interaction time T . But, if T is too long, condition (9) is violated and the derivation of sect. 4 breaks down. We try now to predict what happens when the transverse motion of the atom along the standing wave cannot be neglected. We thus come back to the Fokker–Planck equation (8), keeping now the free flight term.

Suppose first that we neglect the diffusion term in eq. (8). This is equivalent to consider the atomic motion as a classical one and this problem is easily solved from Newton’s equations: for each initial position x , the atom oscillates in the periodic potential U from x to the position symmetrical with respect to the stable equilibrium point (node or antinode of the standing wave depending whether δ is positive or negative).

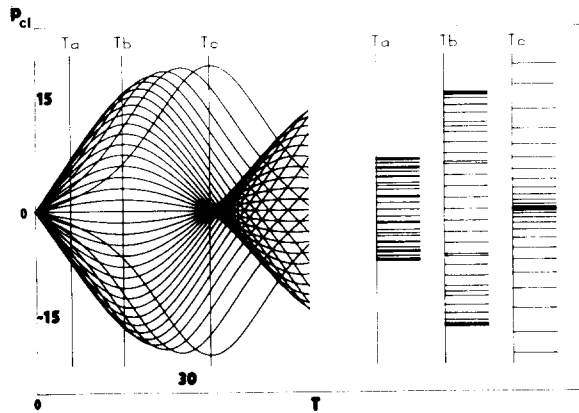


Fig. 3. (a) Set of curves giving the classical momentum $p_{cl}(x_i)$ acquired by an atom entering the standing wave at equally spaced positions x_i . The units are $\hbar k$ for the momentum (vertical axis) and Γ^{-1} for the interaction time (horizontal axis). Parameters are $dE_0/\hbar = 5\Gamma$, $\delta = -5\Gamma$. (b) Distribution of the $p_{cl}(x_i)$ ’s for $T_b = 17.5 \Gamma^{-1}$ (quarter of the oscillation period) and $T_c = 35 \Gamma^{-1}$ (half an oscillation period). The $p_{cl}(x_i)$ ’s bunch near the two extremal values of p_{cl} for T_b , whereas they bunch near $p = 0$ for T_c .

Fig. 3 represents the variation of the classical momentum $p_{cl}(x_i)$ versus the interaction time for equally spaced initial values x_i of x .

For an interaction time T much shorter than the oscillation period (T_a on fig. 3), the $p_{cl}(x_i)$ ’s can be identified with the quantities $\bar{p}(x_i) = Tf(x_i)$ of sect. 4. One thus gets the same conclusions: the deflection profile has a two-peaked structure (in this section, we only consider the non resonant case).

For an interaction time T of the order of a quarter of an oscillation period (T_b on fig. 3), most of the $p_{cl}(x_i)$ ’s reach their maximum values compatible with energy conservation $p^2/2M + U(x) = U(x_i)$. As previously, the $p_{cl}(x_i)$ ’s bunch near two extremal values (fig. 3b). One still expects two-peaked deflection profiles, with now the largest possible structure [of the order of $(2MU_0)^{1/2}$ where U_0 is the potential depth].

On the other hand, for an interaction time T of the order of half an oscillation period (T_c on fig. 3), the $p_{cl}(x_i)$ ’s bunch around $p = 0$ and one expects a single-peaked structure.

A numerical integration of the Fokker–Planck equation (8) has been performed in order to check these qualitative predictions. The computed deflection profile corresponding to T_b is represented on fig. 4 and indeed exhibits a double-peaked structure, whereas the profile corresponding to T_c exhibits a single-peaked one, which confirms the previous discussion.

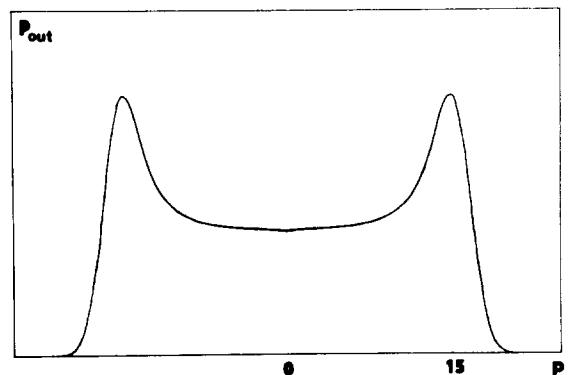


Fig. 4. Deflection profile computed from a numerical integration of the Fokker–Planck equation (the free flight term being taken into account). Same parameters as for fig. 3 with $T = T_b$.

6. Conclusion

We have predicted double-peaked structures in the deflection profile of a monoenergetic atomic beam crossing a laser standing wave slightly detuned from resonance. The experimental observation of such an effect should be possible by using a velocity selected effusive beam or a supersonic beam. The qualitative discussion of section 5 shows that the optimal interaction time is equal to a quarter of the oscillation period in the periodic potential. This corresponds to the maximum value of the deflection angle and to the best contrast for the double-peaked structure.

References

- [1] E. Arimondo, H. Lew and T. Oka, *Phys. Rev. Lett.* 43 (1979) 753.
- [2] F. Viala, Thèse de 3ème cycle, Orsay (1982).
- [3] V.A. Grinchuk, E.F. Kuzin, M.L. Nagaeva, G.A. Ryabenko, A.P. Kazantsev, G.I. Surdutovich and V.P. Yakovlev, *Phys. Lett.* 86 A (1981) 136.
- [4] A.P. Kazantsev, G.I. Surdutovich and V.P. Yakovlev, *Sov. Phys. JETP Lett.* 31 (1980) 509.
- [5] A.P. Kazantsev, G.I. Surdutovich and V.P. Yakovlev, *J. Physique* 42 (1981) 1231; and references therein.
- [6] L. Mandel, *J. Optics (Paris)* 10 (1979) 51.
- [7] R.J. Cook and A.F. Bernhardt, *Phys. Rev. A* 18 (1978) 2533.
- [8] G. Compagno, J.S. Peng and F. Persico, *Phys. Lett.* 88A (1982) 285.
- [9] A.F. Bernhardt and B.W. Shore, *Phys. Rev. A* 23 (1981) 1290.
- [10] E. Arimondo, A. Bambini and S. Stenholm, *Phys. Rev. A* 24 (1981) 898.
- [11] V.S. Letokhov and V.G. Minogin, *Phys. Rep.* 73 (1981) 1 and references therein.
- [12] V.G. Minogin, *Sov. Phys. JETP* 53 (1982) 1164.
- [13] A. Ashkin, *Phys. Rev. Lett.* 40 (1978) 729.
- [14] J.P. Gordon and A. Ashkin, *Phys. Rev. A* 21 (1980) 1606.
- [15] R.J. Cook, *Phys. Rev. Lett.* 44 (1980) 976.
- [16] R.J. Cook, *Comments Atom. Mol. Phys.* 10 (1981) 267.
- [17] S.R. De Groot and L.G. Suttrop, *Foundations of electrodynamics* (North-Holland, 1972).
- [18] R.J. Cook, *Phys. Rev. A* 22 (1980) 1078.
- [19] J. Javanainen and S. Stenholm, *Appl. Phys.* 21 (1980) 35.
- [20] R.L. Liboff, *Introduction to the theory of kinetic equations* (Wiley, New York, 1968).